

# Moral transgressions corrupt neural representations of value

Molly J Crockett<sup>1,2</sup>, Jenifer Z Siegel<sup>1</sup>, Zeb Kurth-Nelson<sup>3,4</sup>, Peter Dayan<sup>5</sup>  & Raymond J Dolan<sup>3,4</sup>

Moral systems universally prohibit harming others for personal gain. However, we know little about how such principles guide moral behavior. Using a task that assesses the financial cost participants ascribe to harming others versus themselves, we probed the relationship between moral behavior and neural representations of profit and pain. Most participants displayed moral preferences, placing a higher cost on harming others than themselves. Moral preferences correlated with neural responses to profit, where participants with stronger moral preferences had lower dorsal striatal responses to profit gained from harming others. Lateral prefrontal cortex encoded profit gained from harming others, but not self, and tracked the blameworthiness of harmful choices. Moral decisions also modulated functional connectivity between lateral prefrontal cortex and the profit-sensitive region of dorsal striatum. The findings suggest moral behavior in our task is linked to a neural devaluation of reward realized by a prefrontal modulation of striatal value representations.

Despite the diversity of human moral values, there is a universal prohibition on harming others for personal gain<sup>1,2</sup>. Humans avoid harming others to a remarkable degree compared with other species<sup>3</sup> and are even willing to incur significant personal costs to alleviate others' suffering<sup>4,5</sup>. Why and how people forgo self-interest for the sake of others' welfare remains an enduring puzzle. Recent work has implicated specific brain regions in moral decision-making<sup>6–9</sup> and probed how moral behavior relates to social cognitive processes such as empathy and mentalizing<sup>10–14</sup>. However, little is known about the neural computations supporting moral decisions to avoid harming others for personal gain and whether individual differences in these computations predict variation in actual moral behavior.

We measured moral behavior in a task where participants could trade personal profit against pain experienced by either themselves or an anonymous other person (Fig. 1a). Most people required more financial compensation to increase others' pain compared with their own<sup>15,16</sup>. In other words, profiting from another's pain had lower subjective value than profiting from one's own pain. One possible explanation for this moral preference is that another's pain is more aversive than one's own pain. Alternatively, profit gained from harming another may engender less pleasure than the very same profit gained from harming oneself<sup>17</sup>.

Because the moral behavior we are interested in here reflects a tradeoff between profit and pain, these competing explanations are not easily resolved from behavioral observation alone. However, using neuroimaging, we can ask whether individual differences in moral preferences are better explained by differential neural representations of pain or profit in the context of harming others versus oneself. Previous neuroimaging studies of moral decision-making have attributed activity in several brain regions to a range of cognitive

processes. Activity in insula, anterior cingulate cortex (ACC) and temporoparietal junction (TPJ) is linked to empathy and mentalizing<sup>7,8,10–14</sup>; activity in striatum and ventromedial prefrontal cortex (vmPFC) is associated with value computation<sup>8,12,13</sup>; and lateral prefrontal cortex (LPFC) activity is considered to reflect cognitive control<sup>6–9</sup>. However, decomposing the cognitive mechanisms supporting moral decisions is difficult without resorting to reverse inference. Here we addressed this challenge by independently manipulating the amounts of profit and pain resulting from participants' decisions (Fig. 1b). This in turn allowed us to extract neural representations of profit and pain and to ask whether the former was suppressed or the latter boosted as a function of the behavioral expression of a moral aversion to harming others for profit. We avoided reverse inference by asking whether, in line with moral behavior, any brain region showed a greater response to others' pain compared to one's own pain or showed a weaker response to profit gained from harming others relative to profit gained from harming oneself. Our prediction, based on prior literature, was that moral decisions involving a tradeoff between pain and profit would engage regions implicated in pain processing or in value-based decision-making, respectively, with pain encoded in insula, ACC and TPJ<sup>18,19</sup> and profit encoded in the striatum and vmPFC<sup>20,21</sup>.

Higher-order goals represented in regions such as LPFC are known to modulate value computations in striatum and vmPFC<sup>22</sup>. In particular, LPFC is implicated in orchestrating the influence of moral norms on behavior<sup>23–29</sup>. This region shows increased activation to the extent that people choose to comply with fairness norms<sup>24</sup>, reciprocate trust<sup>26</sup> and avoid harming others for personal gain<sup>8</sup>. Disrupting LPFC activity impairs the integration of moral blame assessments into punishment decisions<sup>28</sup>. However, notwithstanding these observations, the

<sup>1</sup>Department of Experimental Psychology, University of Oxford, Oxford, UK. <sup>2</sup>Department of Psychology, Yale University, New Haven, Connecticut, USA.

<sup>3</sup>Max Planck–University College London Centre for Computational Psychiatry and Ageing, London, UK. <sup>4</sup>Wellcome Trust Centre for Neuroimaging, University College London, London, UK. <sup>5</sup>Gatsby Computational Neuroscience Unit, University College London, London, UK. Correspondence should be addressed to M.J.C. ([mj.crockett@yale.edu](mailto:mj.crockett@yale.edu)).

Received 13 January; accepted 4 April; published online 1 May 2017; doi:10.1038/nn.4557

precise computational role of LPFC in promoting norm compliance remains unanswered. One proposal is that LPFC regulates moral behavior by reweighting the inputs to policy decisions<sup>30</sup>, for example by modulating the subjective value of harmful actions represented in the striatum<sup>23,31</sup>. This view is grounded in evidence for major anatomical projections from LPFC to dorsal striatum (DS)<sup>32,33</sup> as well as LPFC modulation of DS value signals during temporal discounting<sup>34</sup>. On the bases of these prior data, we hypothesized that value-sensitive areas of DS would show a reduced response to profit gained from harming others, relative to harming oneself, and that moral decisions would modulate functional connectivity between these same value processing regions and LPFC.

We tested our hypotheses in an fMRI study in which participants ( $n = 28$ ) played the role of a ‘decider’ who chose whether to profit by inflicting painful electric shocks on either themselves or on an anonymous other ‘receiver’ (Fig. 1a,b). Crucially, deciders faced identical choice sets when deciding to profit from harm to others versus themselves, enabling us to ask how potential moral transgressions modulate neural representations of profit and pain. To mitigate concerns about reciprocity and reputation, deciders were instructed their choices would be private with respect to the receivers and experimenters, and post-study questionnaires confirmed they believed this. In a second behavioral study involving a similar design we asked participants ( $n = 49$ ) to provide blame judgments in addition to moral decisions (Supplementary Fig. 1). This enabled us to build a model linking blame judgments and moral decisions, which we used to test hypotheses about moral norm representation in LPFC.

## RESULTS

### Computational model of moral decisions

In the moral decision task, we modeled deciders’ choices by adapting a model we had validated in four previous behavioral studies<sup>15,16</sup>. The model again explained the current data well, correctly predicting 87% of deciders’ choices (95% confidence interval (85–88%); mean pseudo- $r^2 = 0.692$ ) and outperformed a range of alternative models (Supplementary Modeling Note). The model described

the difference in subjective value between the harmful and helpful options as follows:

$$\Delta V = (1 - \kappa)\Delta m - \kappa\Delta s$$

$$\kappa = \begin{cases} \kappa_{\text{self}} & \text{if Self trial} \\ \kappa_{\text{other}} & \text{if Other trial} \end{cases}$$

where  $\Delta V$  is the difference in subjective value between the harmful and helpful options, and  $\Delta m$  and  $\Delta s$  are the objective differences in money and shocks between the harmful and helpful options, respectively.  $\Delta V$  is based on a weighted average of these two quantities, in which the relative weighting is determined by a harm-aversion parameter,  $\kappa$ . When  $\kappa = 0$ , deciders will accept any number of shocks to gain profit. As  $\kappa$  approaches 1, deciders become maximally harm-averse and will sacrifice increasing amounts of profit to avoid an additional shock. The setting of  $\kappa$  depends on who is receiving the shocks, where  $\kappa_{\text{self}}$  and  $\kappa_{\text{other}}$  capture the subjective cost of harm to self (Self condition) and others (Other condition), respectively. Trial-by-trial subjective value differences were transformed into choice probabilities using a softmax function<sup>35</sup>. Consistent with previous findings<sup>20,21</sup>, blood-oxygen-level-dependent (BOLD) responses at choice onset correlated with model estimates of the subjective value of the chosen option relative to the unchosen one (relative chosen value; GLM1) in a network including vmPFC ( $P_{\text{FWE}} < 0.0001$ ), mid-posterior cingulate ( $P_{\text{FWE}} < 0.0001$ ), precuneus ( $P_{\text{FWE}} < 0.0001$ ) and bilateral clusters encompassing the amygdala, striatum and insula ( $P_{\text{FWE}} < 0.0001$ ; all results were whole-brain family-wise error (FWE)-corrected at the cluster level after voxel-wise thresholding at  $P < 0.001$ ; Supplementary Fig. 2a and Supplementary Table 1). The relative chosen value signal in these regions did not significantly differ between the Self and Other conditions.

Previous studies using this task showed that most participants displayed moral preferences involving a greater harm aversion for others than for oneself<sup>15,16</sup>. We replicated this effect again in the current study ( $\kappa_{\text{other}} > \kappa_{\text{self}}$ ,  $M = 0.053$ , standard deviation (s.d.) = 0.116,

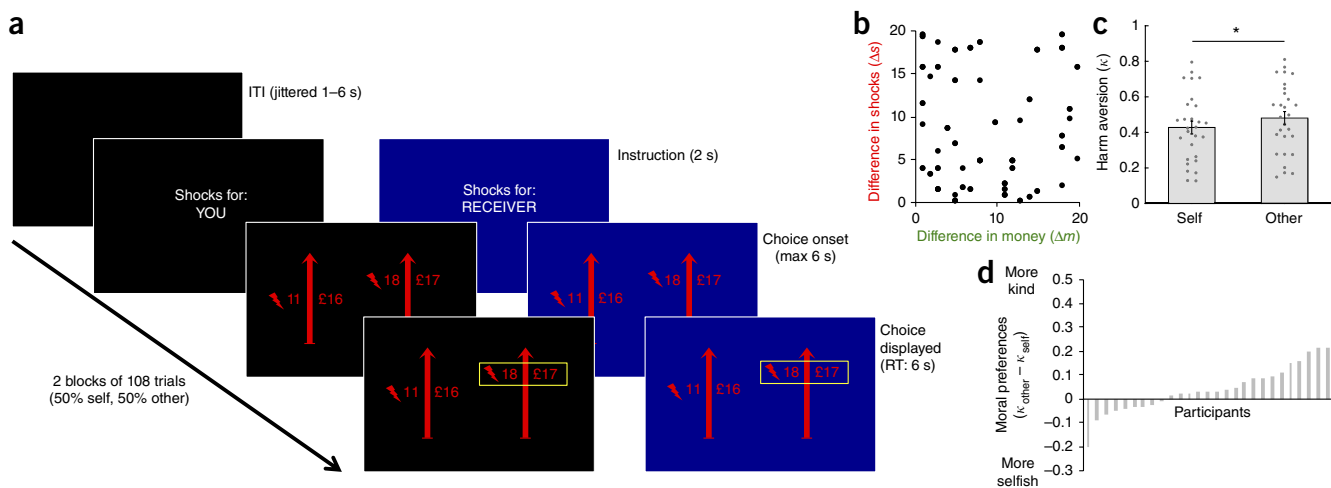


**Figure 1** Moral decision task and behavioral results. **(a)** In the fMRI study, participants assigned to the role of ‘decider’ ( $n = 28$ ) chose between a harmful option containing more money and shocks, and a helpful option containing less money and fewer shocks. The selected option was highlighted by a yellow box. On half the trials the shocks were for the decider (left, black) and on the other half the shocks were for the receiver (right, blue). ITI, intertrial interval. **(b)** Example trial set; each point represents one trial. Across trials, we independently manipulated the difference in pain and difference in profit between the two options, which allowed us to separate neural signals related to pain and profit. **(c)** Harm aversion ( $\kappa$ ) was greater for others than for oneself ( $t_{27} = -2.40$ ,  $P = 0.024$ ). **(d)** Distribution of moral preferences ( $\kappa_{\text{other}} - \kappa_{\text{self}}$ ) among deciders. Error bars depict s.e.m. \* $P < 0.05$ .

$t_{27} = -2.40$ ,  $P = 0.024$ ; **Fig. 1c**). This pattern of moral preferences was observed in 68% of participants (**Fig. 1d**). Analysis of raw choice data indicated that participants were more likely to choose the harmful option for themselves than for the receiver (difference score,  $M = 5\%$ ,  $s.d. = 12\%$ ;  $t_{27} = 2.18$ ,  $P = 0.038$ ). Moral preferences (computed as the difference in harm aversion for self and for others, i.e.,  $\kappa_{\text{other}} - \kappa_{\text{self}}$ ) resulted in participants paying, on average, an extra 17 pence per shock to prevent shocks to others relative to themselves.

Responses in vmPFC reflected these moral preferences. We regressed participant-specific subjective values for the harmful option against BOLD responses at choice onset and extracted the parameter estimates from the value-sensitive vmPFC region identified above. In this region of vmPFC, BOLD responses were less correlated with the value of harming others than the value of harming oneself ( $t_{27} = 2.51$ ,  $P = 0.019$ ; **Supplementary Fig. 2b**). Nevertheless, as seen previously, there was wide individual variation in the degree of expression of moral preferences, which we exploited to probe the neural computations that guide moral decisions.

### Neural representation of profit but not pain predicts moral behavior

Our first aim was to test whether moral behavior is explained by a greater neural sensitivity to anticipated pain for others relative to oneself or by a lesser neural sensitivity to profit gained from harming others relative to harming oneself. We tested these hypotheses in a general linear model (GLM) that identified regions responding parametrically at choice onset, irrespective of participants' decisions, to the objective amounts of profit and pain ( $\Delta m$  and  $\Delta s$ , respectively) that would result from choosing the harmful option, relative to the helpful option, in the Self and Other conditions (GLM2).

For the pain analysis, we identified voxels in which activity varied parametrically with  $\Delta s$ , irrespective of choice. Region-of-interest (ROI) analyses revealed neural responses to  $\Delta s_{\text{self}}$  and  $\Delta s_{\text{other}}$  in ACC and TPJ, respectively, but these were not correlated with individual differences in behavior (**Supplementary Fig. 3**). For completeness, we regressed individual differences in moral preferences onto the group-level maps of parametric responses to anticipated pain for others relative to pain for oneself ( $\Delta s_{\text{other}} > \Delta s_{\text{self}}$ ). In a whole-brain analysis, we found no clusters exceeding a significance level of FWE-corrected  $P < 0.05$  or within any a priori ROIs (**Supplementary Table 2**). Thus, we did not find evidence supporting a relationship between individual differences in univariate neural responses to anticipated pain and variation in moral behavior. Although this null association could reflect an absence of robust neural responses to anticipated pain, this is unlikely, because there was a robust relationship between individual differences in  $\kappa_{\text{self}}$  and neural responses to  $\Delta s_{\text{self}}$  in the insula ( $P_{\text{FWE}} = 0.011$ , whole-brain FWE-corrected at the cluster level after voxel-wise thresholding at  $P < 0.001$ ; **Supplementary Table 3**).

Finally, we investigated a possible relationship between other-related pain signals in TPJ and ACC and choice-related value signals in vmPFC. To test this, we correlated vmPFC responses to the value of harming others (**Supplementary Fig. 2b**) with TPJ and ACC responses to  $\Delta s_{\text{other}}$  (**Supplementary Fig. 3b,e**). The correlations were not significant (vmPFC-TPJ: robust correlation,  $r = -0.04$ , 95% confidence interval (CI) =  $[-0.43, 0.41]$ ; vmPFC-ACC: robust correlation,  $r = -0.02$ , 95% CI =  $[-0.41, 0.40]$ ).

To determine whether moral behavior relates to a differential neural sensitivity to profit gained from harming others versus self, we recapitulated the previous analysis of pain, identifying voxels where activity varied parametrically with  $\Delta m$ , irrespective of choice. We then asked whether these profit-sensitive regions showed differential

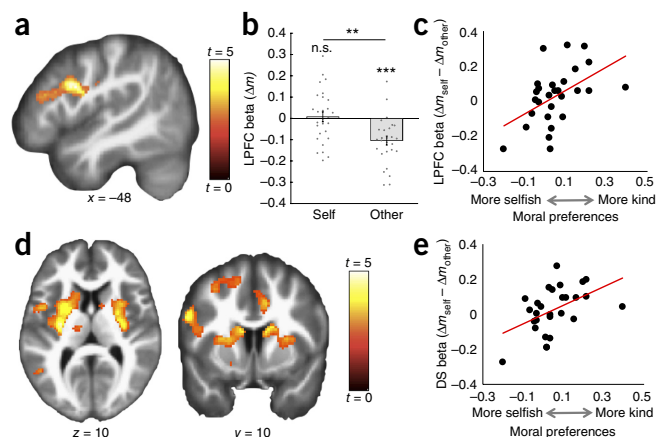


**Figure 2** Moral transgressions modulate corticostriatal responses to profit. **(a)** At choice onset, left LPFC activity negatively correlated with the relative amount of profit gained from harming others relative to oneself ( $\Delta m_{\text{self}} > \Delta m_{\text{other}}$ ;  $P_{\text{FWE}} = 0.027$ , whole-brain FWE-corrected at the cluster level after voxel-wise thresholding at  $P < 0.001$ ). Image displayed at  $P < 0.005$ , uncorrected, to show extent of activation; lighter color indicates greater activation. Coordinates  $x$ ,  $y$ , and  $z$  indicate MNI (Montreal Neurological Institute) coordinates. **(b)** Mean signal from an independently defined ROI in LPFC, separately extracted for the Self and Other conditions, was uncorrelated with  $\Delta m_{\text{self}}$  ( $t_{27} = 0.31$ ,  $P = 0.76$ ) but negatively correlated with  $\Delta m_{\text{other}}$  ( $t_{27} = -4.97$ ,  $P = 0.00003$ ). **(c)** Differential LPFC response to profit gained from harming oneself versus others positively correlated with individual differences in moral preferences (robust correlation,  $r = 0.53$ , 95% CI =  $[0.14, 0.74]$ ). **(d)** A second-level parametric map of moral preferences regressed against the contrast  $\Delta m_{\text{self}} > \Delta m_{\text{other}}$ . For participants showing stronger moral preferences, DS was less responsive to profit gained from harming others than profit gained from harming oneself ( $P_{\text{FWE}} < 0.0001$ , whole-brain FWE-corrected at the cluster level after voxel-wise thresholding at  $P < 0.001$ ). Image displayed at  $P < 0.005$ , uncorrected, to show extent of activation. **(e)** Parameter estimates for  $\Delta m_{\text{other}}$  and  $\Delta m_{\text{self}}$  were extracted from an independently defined ROI in DS. Reduced DS responses to profit gained from harming others (relative to harming oneself) were positively correlated with moral preferences (robust correlation,  $r = 0.49$ , 95% CI =  $[0.20, 0.72]$ ). Error bars depict s.e.m.  $**P < 0.01$ ;  $***P < 0.0001$ ; n.s., nonsignificant.

sensitivity to profit gained from harming others relative to harming oneself ( $\Delta m_{\text{self}} > \Delta m_{\text{other}}$ ). This contrast revealed an effect in left LPFC ( $P_{\text{FWE}} = 0.027$ , whole-brain FWE-corrected at the cluster level after voxel-wise thresholding at  $P < 0.001$ ; **Fig. 2a** and **Supplementary Table 4**). To probe the nature of this effect, we extracted the mean signals from an independently defined ROI in LPFC separately for the Self and Other conditions. This revealed an insensitivity to profit gained from harming oneself ( $\beta_{\Delta m_{\text{self}}} = 0.007 \pm 0.02$ ,  $t_{27} = 0.31$ ,  $P = 0.76$ ; **Fig. 2b**) but a negative parametric response in LPFC to profit gained from harming others ( $\beta_{\Delta m_{\text{other}}} = -0.10 \pm 0.02$ ;  $t_{27} = -4.97$ ,  $P = 0.00003$ ). The LPFC response to ill-gotten gains did not significantly differ on trials in which participants chose to harm versus help others ( $t_{27} = 0.16$ ,  $P = 0.87$ ). The differential response in LPFC to profit gained from harming others versus oneself was more pronounced as a function of the strength of expressed moral preferences, with more moral participants showing a stronger differential response to profit from self- versus other-harm in LPFC (robust correlation,  $r = 0.53$ , 95% CI =  $[0.14, 0.74]$ ; **Fig. 2c**).

We then asked whether there were additional regions expressing differential activity for profit gained from harming oneself versus others, which in turn correlated with moral preferences. We regressed individual differences in moral preferences onto the group-level

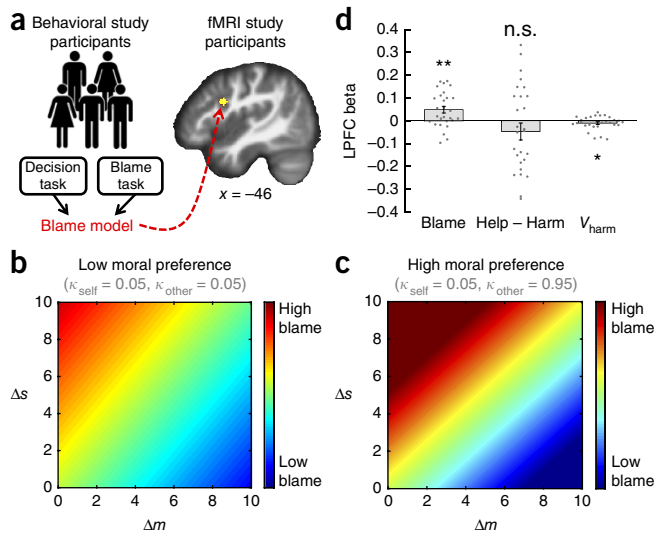


**Figure 3** Blame computation in LPFC. (a) Behavioral study participants ( $n = 49$ ) completed a moral decision task and a moral blame task. These data were used to construct a model of blame, which we used to create a unique blame trajectory for each participant in the fMRI study ( $n = 28$ ). We then regressed these blame estimates against activity in an independently defined ROI in LPFC (yellow sphere). (b,c) Model estimates of blame as a function of profit ( $\Delta m$ ) and pain ( $\Delta s$ ) for a participant with (b) low and (c) high moral preferences. Across all participants, blame was highest for choices inflicting high pain for low profit. (d) LPFC signal was positively correlated with blame (GLM5;  $t_{27} = 2.89$ ,  $P = 0.007$ ); did not significantly differ for helpful vs. harmful choices (GLM5;  $t_{27} = -0.96$ ,  $P = 0.35$ ); and was negatively correlated with the subjective value of the harmful option,  $V_{\text{harm}}$  (GLM6;  $t_{27} = -2.21$ ,  $P = 0.04$ ). Error bars depict s.e.m. \* $P < 0.05$ ; \*\* $P < 0.01$ ; n.s., nonsignificant.

maps of the parametric response to profiting from harming oneself relative to others ( $\Delta m_{\text{self}} > \Delta m_{\text{other}}$ ). In addition to the previously observed effect in LPFC, we observed a robust effect in bilateral DS extending into the insula ( $P_{\text{FWE}} < 0.0001$ ), superior temporal gyrus ( $P_{\text{FWE}} = 0.007$ ), posterior cingulate ( $P_{\text{FWE}} < 0.0001$ ) and posterior medial PFC ( $P_{\text{FWE}} = 0.0003$ ); all results whole-brain FWE-corrected at the cluster level after voxel-wise thresholding at  $P < 0.001$ ; **Fig. 2d** and **Supplementary Table 5**). This network overlapped substantially with regions in which activity correlated with relative chosen value (conjunction analysis,  $P_{\text{FWE}} < 0.0001$ , whole-brain FWE-corrected at the cluster level after voxel-wise thresholding at  $P < 0.001$ ; **Supplementary Table 6**). Furthermore, other-related profit signals in DS were significantly correlated with relative chosen value signals in vmPFC (robust correlation,  $r = 0.40$ , 95% CI = [0.02, 0.77]).

To further investigate the relationship between moral preferences and DS responses to profit, we examined parametric responses in DS (mean signal extracted from independently defined ROI) to the amount of profit gained from harming oneself and others separately. Moral participants ( $\kappa_{\text{other}} > \kappa_{\text{self}}$ ) showed positive parametric responses in DS to the amount of profit gained from harming oneself ( $\beta_{\Delta m_{\text{self}}} = 0.05 \pm 0.02$ ,  $t_{17} = 2.60$ ,  $P = 0.018$ ) but not to profit gained from harming others ( $\beta_{\Delta m_{\text{other}}} = 0.004 \pm 0.03$ ,  $t_{17} = 0.15$ ,  $P = 0.88$ ), and the reductions we observed in DS responses to profit gained from harming others (relative to harming oneself) correlated positively with moral preferences (robust correlation,  $r = 0.49$ , 95% CI = [0.20, 0.72]; **Fig. 2e**). This suggests moral behavior might arise via an attenuation of DS responses to profit gained from harming others.

### Computation of moral value in LPFC

During moral decision-making, LPFC responded more strongly during trials in which participants could harm others for a small profit, relative to trials in which harming others resulted in a larger profit. A similar pattern has been reported for blame judgments; blame is higher for moral transgressions resulting in lower profit<sup>36</sup>. Thus, people may anticipate more blame for harmful decisions yielding lower profit, and this anticipated blame could be encoded by LPFC, in line with previous work showing LPFC responses to moral norm violations<sup>24–30</sup>. Directly testing this hypothesis required us to construct, for each participant, a trial-by-trial trajectory of anticipated blame and regress this against LPFC activity. Although participants in the fMRI study did not provide blame judgments, we hypothesized that, within our study population, blame could be predicted based on choice features ( $\Delta m$ ,  $\Delta s$ ) and individual preferences ( $\kappa_{\text{self}}$ ,  $\kappa_{\text{other}}$ ). This allowed us to infer blame judgments for the fMRI participants from a model of blame built using data from a separate group of participants who provided blame judgments in addition to moral decisions (**Fig. 3a**).

The model described blame judgments as follows:

$$\text{Blame}_t = \beta_0 + \beta_1 \Delta m_t + \beta_2 \Delta s_t + \beta_3 \Delta m_t \kappa_o + \beta_4 \Delta m_t \kappa_s + \beta_5 \Delta s_t \kappa_o + \beta_6 \Delta s_t \kappa_s + \beta_7 \Delta m_t \kappa_o \kappa_s + \beta_8 \Delta s_t \kappa_o \kappa_s$$

where blame on trial  $t$  is a linear function of choice features on trial  $t$  ( $\Delta m_t$ ,  $\Delta s_t$ ), individual preferences ( $\kappa_s$ ,  $\kappa_o$ ) and their interactive combinations (see **Supplementary Modeling Note** for parameter estimates; mean  $r^2 = 0.33$ ). Blame was negatively correlated with profit ( $\beta_1 = -0.07$ , 95% CI = [-0.10, -0.04]) and positively correlated with pain ( $\beta_2 = 0.05$ , 95% CI = [0.01, 0.09]). Individual preferences modulated the relationship between profit, pain and blame such that participants with stronger moral preferences showed more extreme judgments and a stronger influence of pain (relative to money) on blame (**Fig. 3b,c**).

Next, we performed multiple regression on the BOLD signal extracted from an independently defined ROI in LPFC. Using the blame model described above, we constructed a trajectory of anticipated blame for each fMRI participant and then tested whether LPFC signal correlated with anticipated blame estimates in a GLM that included anticipated blame, relative chosen value and total value, which were orthogonalized (GLM3). This analysis showed a positive correlation between LPFC activity and anticipated blame ( $t_{27} = 2.67$ ,  $P = 0.012$ ). The relationship between LPFC activity and anticipated blame remained significant when controlling for the total amounts of money and shocks on each trial (GLM4;  $t_{27} = 2.84$ ,  $P = 0.008$ ). If LPFC computes anticipated blame to guide decision-making, this value should be choice-independent. Consistent with this, the relationship between LPFC and blame did not differ significantly on trials in which participants harmed versus helped others ( $t_{27} = -0.86$ ,  $P = 0.40$ ).

An alternative account of LPFC function in prosocial behavior is that this region serves a role akin to a ‘brake system’ for inhibiting self-interested behavior, i.e., influencing policy selection once values are computed<sup>31,37</sup>. To rule out this account, we conducted several analyses, focusing on trials in the Other condition. First, we examined participants’ response times (RTs). If choosing the helpful option involves an inhibition of self-interest, then helpful choices should be slower than harmful choices (RT-GLM1; **Supplementary Table 7**). In fact, RTs were faster for helpful relative to harmful choices ( $t_{27} = -3.76$ ,  $P = 0.0008$ ). RT data actually supported a blame computation account. If moral choices involve integrating moral value into overall subjective value, people with stronger moral preferences should respond more slowly in the Other condition (in which moral values must be

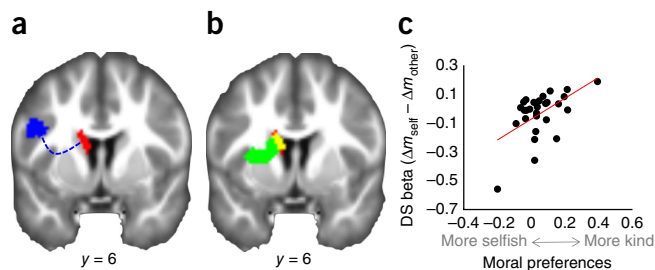


**Figure 4** Corticostriatal connectivity during the exercise of moral choices. **(a)** Moral decisions modulated functional connectivity between seed region in LPFC (blue) and DS (red). Red cluster in DS ( $P_{FWE} = 0.025$ , whole-brain FWE-corrected at the cluster level after voxel-wise thresholding at  $P < 0.001$ ) depicts conjunction of PPI contrasts [LPFC seed  $\times$  help-other  $>$  harm-other] and [LPFC seed  $\times$  help-other  $>$  help-self]. Image displayed at  $P < 0.005$ , uncorrected, to show extent of activation. **(b)** The area of DS showing differential functional connectivity with LPFC during moral decisions (red) overlapped considerably with the area of DS showing reduced responses to profit gained from harming others vs. harming oneself (green; overlap shown in yellow). Image displayed at  $P < 0.005$ , uncorrected, to show extent of activation. **(c)** Within the area of DS showing differential functional connectivity with LPFC during moral decisions (red cluster), reduced responses to profit gained from harming others (relative to harming oneself) predicted moral preferences (robust correlation,  $r = 0.36$ , 95% CI = [0.002, 0.68]).

computed) than in the Self condition (which requires no such computation). We tested this by comparing RTs for Other versus Self trials in a second GLM (RT-GLM2; **Supplementary Table 7**) and found slowing in the Other condition relative to the Self condition was indeed positively correlated with moral preferences (robust correlation,  $r = 0.52$ , 95% CI = [0.11, 0.80]).

Next, we tested whether LPFC activity differed for harm versus help trials. If LPFC is involved in inhibiting self-interest, then LPFC activity should be higher on ‘successful inhibition’ trials, i.e., trials in which participants chose the helpful option. Because participants were more likely to choose the helpful option on trials where harming would result in more blame ( $t_{27} = 54.29$ ,  $P = 4 \times 10^{-29}$ ), we controlled for blame as well as for relative chosen value and total value (GLM5). We found no difference in LPFC activity between help trials and harm trials ( $t_{27} = -0.96$ ,  $P = 0.35$ ), while the effect of blame on LPFC activity remained significant ( $t_{27} = 2.89$ ,  $P = 0.007$ ; **Fig. 3d**). Finally, we tested whether LPFC responses on help trials depended on the value of the harmful option (GLM6). If LPFC is required for inhibiting self-interest, it should be more active on trials where helping is more difficult (i.e., when the value of the harmful option is high). In fact, LPFC was not more active on helpful trials when the value of the harmful option was high (help  $\times$   $V_{\text{harm}}$  interaction,  $t_{27} = -1.67$ ,  $P = 0.11$ ). Rather, LPFC was less active on trials in which the value of the harmful option was high, regardless of whether participants harmed or helped ( $V_{\text{harm}}$  main effect,  $t_{27} = -2.21$ ,  $P = 0.04$ ; **Fig. 3d**). Thus, our findings are not consistent with the notion that moral behavior involves an inhibition of self-interest implemented by LPFC or indeed anywhere else in the brain.

#### Moral decisions modulate corticostriatal connectivity

Moral preferences were associated with reduced striatal responses to profit from harming others, relative to harming oneself, while LPFC responses correlated with model estimates of blame. This suggests that LPFC may modulate DS responses to profit in line with anticipated blame. This would predict that LPFC should show differential functional connectivity with DS during decisions to help others, compared

with during decisions to harm others and decisions to help oneself. Consequently, we implemented psychophysiological interaction (PPI) analyses with LPFC as a seed region. The PPI models included regressors for the main effect of LPFC activity, the main effect of decision type and their interaction. We examined two decision types in two separate PPI models: (i) helpful choices in the Other condition relative to harmful choices in the Other condition (help-other  $>$  harm-other) and (ii) helpful choices in the Other condition relative to helpful choices in the Self condition (help-other  $>$  help-self). This analysis revealed differential functional connectivity between LPFC and DS during help-other choices relative to harm-other choices and help-self choices (conjunction of contrasts i and ii:  $P_{FWE} = 0.025$ , whole-brain FWE-corrected at the cluster level after voxel-wise thresholding at  $P < 0.001$ ; **Fig. 4a**, **Supplementary Fig. 4a** and **Supplementary Table 8**). This region overlapped with the cluster in DS identified above as showing differential responses to profit from harming self versus others as a function of moral preferences (**Fig. 4b**). The results are consistent with a model whereby LPFC modulates DS responses to profit in line with moral considerations.

Participants with stronger moral preferences showed a greater reduction in the DS response to profit gained from harming others relative to harming oneself. If translating moral norms into moral behavior involves changes in functional connectivity between LPFC and DS, then we should also see a relationship between moral preferences and reduced responses to profiting from others’ pain in the precise area of DS that was functionally connected with LPFC. To test this hypothesis, we extracted, for each participant, the contrast estimate ( $\Delta m_{\text{self}} > \Delta m_{\text{other}}$ ) from the DS cluster identified in the PPI analysis and regressed these estimates against participants’ moral preferences. This analysis revealed a positive correlation between moral preferences and reductions in the DS response to profiting from harming others relative to harming oneself (robust correlation,  $r = 0.36$ , 95% CI = [0.002, 0.68]; **Fig. 4c**). That is, moral decisions modulated functional connectivity between LPFC and DS, and moral preferences were predicted by the extent to which the DS showed a reduced response to profiting from others’ pain relative to one’s own pain.

We next tested whether corticostriatal connectivity was associated with choice-related striatal value signals. As an index of value sensitivity in DS, we extracted, for each participant, the mean signal from the voxels in DS that were sensitive to relative chosen value ( $t_{27} = 3.28$ ,  $P = 0.003$ ). As an index of corticostriatal connectivity during helpful moral choices, we extracted from this same region of DS the signal from the PPI contrast LPFC  $\times$  help-other. Choice-related value signals in DS were negatively correlated with corticostriatal connectivity (robust correlation,  $r = -0.51$ , 95% CI = [-0.73, -0.14]; **Supplementary Fig. 4b**), suggesting a negative connectivity between LPFC and DS during moral decisions as a function of value sensitivity in DS.

#### DISCUSSION

We offer an account of how a moral prohibition against harming others is translated into moral behavior. Replicating previous findings<sup>15,16</sup>, we showed that most people prefer to harm themselves over others for profit. This moral preference was associated with diminished neural responses in value-sensitive regions to profit accrued from harming others. This observation suggests a neural explanation for why people are reluctant to seek profits from immoral actions<sup>15–17</sup> and disapprove of individuals and organizations who accept money from morally tainted sources<sup>36,38</sup> by revealing that moral transgressions corrupt neural representations of value.

Our findings implicate LPFC in computing the moral value of actions to guide moral decision-making. LPFC negatively encoded

the magnitude of profit gained from harming others but not profit gained from harming oneself, and the strength of this encoding predicted individual differences in moral behavior. LPFC was most active on trials in which inflicting pain yielded minimal profit, the very same trials considered most blameworthy by a second group of participants who provided blame judgments of decisions to harm others for profit. A model of blame built from these judgments predicted LPFC activity in fMRI participants, consistent with a role for LPFC in representing moral values.

Previous accounts of LPFC in prosocial behavior have distinguished between inhibitory ‘braking’ functions and executive ‘overriding’ functions, generally attributed to more ventral and more dorsal aspects of LPFC, respectively<sup>39</sup>. The region we observed here, situated in the inferior frontal gyrus, did not show activity consistent with inhibitory control. It was not more active during helpful decisions than harmful decisions or when helpful choices were more difficult. Instead, its activity pattern suggested an encoding of moral goals, which may be used to modulate action values represented in DS<sup>23,31</sup>. This mechanism has parallels with models of self-control in nonsocial decision-making, whereby long-term goals represented in LPFC modulate neural representations of value<sup>22,34</sup>.

We tested this hypothesis with functional connectivity analyses and found a more negative connectivity between LPFC and DS during the exercise of helpful choices compared to harmful choices or nonsocial choices. The DS, in turn, showed reduced responses to profit from harming others to the extent that people behaved morally. The connectivity findings suggest two possible mechanisms that are not mutually exclusive. First, they could reflect negative corticostriatal connectivity during helpful decisions, which would suggest that LPFC directly downregulates value representations in DS at the time of choice<sup>34</sup>. Alternatively, they could reflect a greater positive connectivity during harmful decisions than during helpful decisions, which could result from LPFC updating action-value representations in DS following perceived moral transgressions. This latter account follows recent work suggesting that people are uncertain about their preferences and use social information to ‘learn’ what to want<sup>40</sup>. Our data are agnostic on this point as our study was not designed to arbitrate between these mechanisms, but future studies could usefully investigate possible links between moral decision-making and moral learning, including the question of whether harm aversion declines over time<sup>41</sup>. We acknowledge that our conclusions are limited by the correlational nature of neuroimaging findings and suggest that future studies employ brain stimulation or lesion-deficit analyses to deduce the causal role of LPFC in blame computation beyond domain-general attentional or control functions.

We previously reported that acutely enhancing dopamine levels with the dopamine precursor levodopa disrupted moral preferences<sup>16</sup>. The current findings hint at a possible mechanism for this effect. Moral preferences were associated with reduced DS responses to profit gained from harming others relative to self, and this region showed differential functional connectivity with the LPFC during moral decisions. Levodopa may disrupt this corticostriatal circuit by amplifying phasic dopamine signals in the striatum that guide action selection<sup>42,43</sup>, biasing choice toward immediate rewards (i.e., profits) and away from higher-order values (i.e., norm compliance). Such a mechanism would be consistent with reports that antisocial and aggressive behaviors are associated with heightened striatal dopamine<sup>44,45</sup>.

Univariate neural representations of others’ pain during moral decision-making did not correlate with moral preferences in our study. Although previous work has argued such representations play a prominent role in mediating moral behavior<sup>10,14</sup>, these conclusions focused

on neural responses to observing others in pain, rather than neural computations during moral decision-making. As neural representations of others’ pain have been linked to empathy<sup>18,19</sup>, our study informs current debates on the extent to which empathy guides moral behavior<sup>46</sup> and highlights the importance of norms in restraining self-interest. Our findings suggest that neural responses elicited by the potential suffering of anonymous strangers may be dissociated from the moral choices people make, in line with evidence that empathy and a motivation to help others are psychologically distinct<sup>46</sup> and the latter (but not the former) predicts LPFC responses during costly altruism<sup>8</sup>.

Finally, our results shed light on the question of whether moral decisions engage a specialized set of neural computations or simply rely on the same circuitry that is involved in generic value-based decision-making. Previous studies have shown that moral judgments and decisions engage similar neural circuitry as observed for simple value-based decisions<sup>47</sup>, but the encoding of subjective value for moral decision and for decisions without a moral component had never been directly compared in the same study. Here we found that the overall subjective value of moral choices was ultimately reflected in the same regions that encoded the subjective value of non-social choices. Moral preferences were reflected in a reduced vmPFC response to the value of harming others, which could reflect either a directly reduced utility for ill-gotten gains or a partially corrupted mapping of utility onto vmPFC signal for ill-gotten gains. However, we also observed profit-related computations in the LPFC during moral decision-making that were not observed during choices of a similar nature that did not involve a moral component. Responses to ill-gotten gains in LPFC correlated with moral preferences, and this region expressed altered functional connectivity with value-encoding regions during moral choices relative to during choices not involving moral preferences. Thus, the construction of moral values seems to incorporate additional computations that may represent anticipated or internalized moral judgments of others. In this way, our conscience, the “great judge and arbiter of our conduct,”<sup>2</sup> may influence the values that guide the choices we make.

## METHODS

Methods, including statements of data availability and any associated accession codes and references, are available in the [online version of the paper](#).

*Note: Any Supplementary Information and Source Data files are available in the online version of the paper.*

## ACKNOWLEDGMENTS

We thank E. Boorman, A. de Berker, L. Hunt, M. Klein-Flügge, C. Mathys, R. Rutledge, B. Seymour, P. Smittenaar, G. Story, I. Vlaev and J. Winston for feedback. M.J.C. was supported by a Sir Henry Wellcome Postdoctoral Fellowship (092217/Z/10/Z) and a Wellcome Trust Institutional Strategic Support Fund grant. J.Z.S. was supported by a Wellcome Trust Society and Ethics studentship (104980/Z/14/Z). Z.K.-N. was supported by a Joint Initiative on Computational Psychiatry and Ageing Research between the Max Planck Society and University College London. P.D. is funded by the Gatsby Charitable Foundation. R.J.D. holds a Wellcome Trust Senior Investigator Award (098362/Z/12/Z). The Max Planck UCL Centre is a joint initiative supported by UCL and the Max Planck Society. The Wellcome Trust Centre for Neuroimaging, where scanning was carried out, is supported by core funding from the Wellcome Trust (091593/Z/10/Z).

## AUTHOR CONTRIBUTIONS

M.J.C. conceived the study. M.J.C., J.Z.S., Z.K.-N., P.D. and R.J.D. designed the study. M.J.C. and J.Z.S. collected behavioral and fMRI data. M.J.C., J.Z.S., Z.K.-N. and P.D. analyzed the data. M.J.C. wrote the manuscript with edits from J.Z.S., Z.K.-N., P.D. and R.J.D.

## COMPETING FINANCIAL INTERESTS

The authors declare no competing financial interests.

Reprints and permissions information is available online at <http://www.nature.com/reprints/index.html>. Publisher's note: Springer Nature remains neutral with regard to jurisdictional claims in published maps and institutional affiliations.

1. Gert, B. *Common Morality: Deciding What to Do* (Oxford University Press, 2004).
2. Smith, A. *The Theory of Moral Sentiments* (Penguin, 2010).
3. Boehm, C. *Moral Origins: The Evolution of Virtue, Altruism, and Shame* (Basic Books, 2012).
4. Rand, D.G. & Epstein, Z.G. Risking your life without a second thought: intuitive decision-making and extreme altruism. *PLoS One* **9**, e109687 (2014).
5. Marsh, A.A. *et al.* Neural and cognitive characteristics of extraordinary altruists. *Proc. Natl. Acad. Sci. USA* **111**, 15036–15041 (2014).
6. Greene, J.D. in *The Cognitive Neurosciences V* 1013–1023 (MIT Press, 2014).
7. FeldmanHall, O. *et al.* Differential neural circuitry and self-interest in real vs hypothetical moral decisions. *Soc. Cogn. Affect. Neurosci.* **7**, 743–751 (2012).
8. FeldmanHall, O., Dalgleish, T., Evans, D. & Mobbs, D. Empathic concern drives costly altruism. *Neuroimage* **105**, 347–356 (2015).
9. Greene, J.D. & Paxton, J.M. Patterns of neural activity associated with honest and dishonest moral decisions. *Proc. Natl. Acad. Sci. USA* **106**, 12506–12511 (2009).
10. Yu, H., Hu, J., Hu, L. & Zhou, X. The voice of conscience: neural bases of interpersonal guilt and compensation. *Soc. Cogn. Affect. Neurosci.* **9**, 1150–1158 (2014).
11. Morishima, Y., Schunk, D., Bruhin, A., Ruff, C.C. & Fehr, E. Linking brain structure and activation in temporoparietal junction to explain the neurobiology of human altruism. *Neuron* **75**, 73–79 (2012).
12. Hutcherson, C.A., Bushong, B. & Rangel, A. A neurocomputational model of altruistic choice and its implications. *Neuron* **87**, 451–462 (2015).
13. Hare, T.A., Camerer, C.F., Knoepfle, D.T. & Rangel, A. Value computations in ventral medial prefrontal cortex during charitable decision making incorporate input from regions involved in social cognition. *J. Neurosci.* **30**, 583–590 (2010).
14. Hein, G., Silani, G., Preuschoff, K., Batson, C.D. & Singer, T. Neural responses to ingroup and outgroup members' suffering predict individual differences in costly helping. *Neuron* **68**, 149–160 (2010).
15. Crockett, M.J., Kurth-Nelson, Z., Siegel, J.Z., Dayan, P. & Dolan, R.J. Harm to others outweighs harm to self in moral decision making. *Proc. Natl. Acad. Sci. USA* **111**, 17320–17325 (2014).
16. Crockett, M.J. *et al.* Dissociable effects of serotonin and dopamine on the valuation of harm in moral decision-making. *Curr. Biol.* **25**, 1852–1859 (2015).
17. Stellar, J.E. & Willer, R. The corruption of value negative moral associations diminish the value of money. *Soc. Psychol. Personal. Sci.* **5**, 60–66 (2014).
18. Zaki, J. & Ochsner, K.N. The neuroscience of empathy: progress, pitfalls and promise. *Nat. Neurosci.* **15**, 675–680 (2012).
19. Lamm, C., Decety, J. & Singer, T. Meta-analytic evidence for common and distinct neural networks associated with directly experienced pain and empathy for pain. *Neuroimage* **54**, 2492–2502 (2011).
20. Bartra, O., McGuire, J.T. & Kable, J.W. The valuation system: a coordinate-based meta-analysis of BOLD fMRI experiments examining neural correlates of subjective value. *Neuroimage* **76**, 412–427 (2013).
21. Clithero, J.A. & Rangel, A. Informatic parcellation of the network involved in the computation of subjective value. *Soc. Cogn. Affect. Neurosci.* **9**, 1289–1302 (2014).
22. Rangel, A. & Hare, T. Neural computations associated with goal-directed choice. *Curr. Opin. Neurobiol.* **20**, 262–270 (2010).
23. Buckholtz, J.W. & Marois, R. The roots of modern justice: cognitive and neural foundations of social norms and their enforcement. *Nat. Neurosci.* **15**, 655–661 (2012).
24. Spitzer, M., Fischbacher, U., Herrnberger, B., Grön, G. & Fehr, E. The neural signature of social norm compliance. *Neuron* **56**, 185–196 (2007).
25. Ruff, C.C., Ugazio, G. & Fehr, E. Changing social norm compliance with noninvasive brain stimulation. *Science* **342**, 482–484 (2013).
26. Chang, L.J., Smith, A., Dufwenberg, M. & Sanfey, A.G. Triangulating the neural, psychological, and economic bases of guilt aversion. *Neuron* **70**, 560–572 (2011).
27. Baumgartner, T., Knoch, D., Hotz, P., Eisenegger, C. & Fehr, E. Dorsolateral and ventromedial prefrontal cortex orchestrate normative choice. *Nat. Neurosci.* **14**, 1468–1474 (2011).
28. Buckholtz, J.W. *et al.* From blame to punishment: disrupting prefrontal cortex activity reveals norm enforcement mechanisms. *Neuron* **87**, 1369–1380 (2015).
29. Treadway, M.T. *et al.* Corticolimbic gating of emotion-driven punishment. *Nat. Neurosci.* **17**, 1270–1275 (2014).
30. Knoch, D., Pascual-Leone, A., Meyer, K., Treyer, V. & Fehr, E. Diminishing reciprocal fairness by disrupting the right prefrontal cortex. *Science* **314**, 829–832 (2006).
31. Buckholtz, J.W. Social norms, self-control, and the value of antisocial behavior. *Curr. Opin. Behav. Sci.* **3**, 122–129 (2015).
32. Haber, S.N., Kim, K.-S., Maily, P. & Calzavara, R. Reward-related cortical inputs define a large striatal region in primates that interface with associative cortical connections, providing a substrate for incentive-based learning. *J. Neurosci.* **26**, 8368–8376 (2006).
33. Choi, E.Y., Yeo, B.T.T. & Buckner, R.L. The organization of the human striatum estimated by intrinsic functional connectivity. *J. Neurophysiol.* **108**, 2242–2263 (2012).
34. van den Bos, W., Rodriguez, C.A., Schweitzer, J.B. & McClure, S.M. Connectivity strength of dissociable striatal tracts predict individual differences in temporal discounting. *J. Neurosci.* **34**, 10298–10310 (2014).
35. Daw, N.D. in *Decision Making, Affect, and Learning: Attention and Performance XXIII* (eds. Delgado, M.R., Phelps, E.A. & Robbins, T.W.) (Oxford University Press, 2011).
36. Xie, W., Yu, B., Zhou, X., Sedikides, C. & Vohs, K.D. Money, moral transgressions, and blame. *J. Consum. Psychol.* **24**, 299–306 (2014).
37. Dolan, M. The neuropsychology of prefrontal function in antisocial personality disorder offenders with varying degrees of psychopathy. *Psychol. Med.* **42**, 1715–1725 (2012).
38. Inbar, Y., Pizarro, D.A. & Cushman, F. Benefiting from misfortune: when harmless actions are judged to be morally blameworthy. *Pers. Soc. Psychol. Bull.* **38**, 52–62 (2012).
39. Feng, C., Luo, Y.-J. & Krueger, F. Neural signatures of fairness-related normative decision making in the ultimatum game: a coordinate-based meta-analysis. *Hum. Brain Mapp.* **36**, 591–602 (2015).
40. Moutoussis, M., Dolan, R.J. & Dayan, P. How people use social information to find out what to want in the paradigmatic case of inter-temporal preferences. *PLOS Comput. Biol.* **12**, e1004965 (2016).
41. Garrett, N., Lazzaro, S.C., Ariely, D. & Sharot, T. The brain adapts to dishonesty. *Nat. Neurosci.* **19**, 1727–1732 (2016).
42. Tai, L.-H., Lee, A.M., Benavidez, N., Bonci, A. & Wilbrecht, L. Transient stimulation of distinct subpopulations of striatal neurons mimics changes in action value. *Nat. Neurosci.* **15**, 1281–1289 (2012).
43. Macpherson, T., Morita, M. & Hikida, T. Striatal direct and indirect pathways control decision-making behavior. *Front. Psychol.* **5**, 1301 (2014).
44. Buckholtz, J.W. *et al.* Mesolimbic dopamine reward system hypersensitivity in individuals with psychopathic traits. *Nat. Neurosci.* **13**, 419–421 (2010).
45. Couppis, M.H., Kennedy, C.H. & Stanwood, G.D. Differences in aggressive behavior and in the mesocorticolimbic DA system between A/J and BALB/c mice. *Synapse* **62**, 715–724 (2008).
46. Jordan, M.R., Amir, D. & Bloom, P. Are empathy and concern psychologically distinct? *Emotion* **16**, 1107–1116 (2016).
47. Ruff, C.C. & Fehr, E. The neurobiology of rewards and values in social decision making. *Nat. Rev. Neurosci.* **15**, 549–562 (2014).

## ONLINE METHODS

**Participants.** Healthy volunteers were recruited from the University College London (UCL) Psychology Department and the Institute of Cognitive Neuroscience subject pools. Exclusion criteria included a history of systemic or neurological disorders, psychiatric disorders, psychoactive medication or drug use, pregnancy, more than two years' study of psychology, and previous participation in studies involving social interactions and/or electric shocks. For the fMRI study, we recruited right-handed participants only.

For the fMRI study, we recruited 37 pairs of participants, with one participant in each pair completing a moral decision task in the fMRI scanner. No statistical methods were used to predetermine sample sizes, but our sample size was based on estimated effect size for moral preferences observed in two previous behavioral studies using the same task<sup>15</sup>. Two participants indicated they did not find the shocks aversive, three participants fell asleep in the scanner, one participant failed to follow task instructions, one participant expressed doubts as to whether the receiver would receive the shocks and one participant requested to exit the scanner during the first run. A power cut resulted in data loss for another participant. These participants were excluded from further analysis, leaving a total of 28 participants in the role of decider whose data were analyzed for the fMRI study (16 males; mean age 21.9 years).

For the behavioral study, 54 participants participated in the role of decider. These participants completed the moral blame task after completing a moral decision task similar to the fMRI task; moral decision data from these participants has been published previously<sup>15</sup>. Five participants did not provide sufficient variation in their blame judgments to allow for model fitting (more than 75% identical judgments or a s.d. in judgments < 0.03); these participants were excluded from further analysis, leaving a total of 49 participants whose data were analyzed for the behavioral study (18 males; mean age 23 years).

**Procedure.** Both studies took place at the Wellcome Trust Centre for Neuroimaging in London and were approved by the UCL Research Ethics Committee (4418/001). Participants completed a battery of online trait questionnaires approximately 1 week before attending a single testing session. Two individuals participated in each session. They arrived at staggered times and were led to separate testing rooms without seeing one another to ensure complete anonymity.

In both studies, after providing informed consent, participants completed a pain thresholding procedure that has been described in detail elsewhere<sup>15</sup>. This procedure allowed us to (i) control for heterogeneity of skin resistance between participants, thus enabling us to deliver shocks of matched subjective intensity to different participants; (ii) administer a range of potentially painful stimuli in an ethical manner during the task itself; and (iii) provide participants with experience of the shocks before the decision task. Participants were then randomly assigned to roles of either decider or receiver using a role assignment procedure that has been described in detail elsewhere<sup>15</sup>.

In the fMRI study, following role assignment, the decider participant completed the moral decision task in the fMRI scanner. In the behavioral study, following role assignment, the decider participant completed the moral decision task, followed by the moral blame task. Deciders were informed that their choices and identity would be kept confidential to minimize the extent to which their choices would be based on concerns about reputation or reciprocity.

After completing the decision task, decider participants completed self-report measures concerning their experiences during the experiment, including a measure of how morally conflicted they felt about their decisions (rated on a 7-point Likert scale, where 1 = 'not at all', 7 = 'very much'). At the end of the session, one trial was randomly selected and actually implemented. Before departing the laboratory all participants completed debriefing questionnaires that assessed their beliefs about the experimental setup, including a measure of confidence that their choices and identity would remain confidential (rated from 1 = 'fully' to 5 = 'not at all'). Participants reported maximal confidence (decisions confidential:  $M = 1.04$ , s.e.m. = 0.04; identity confidential:  $M = 1.04$ , s.e.m. = 0.04). Finally, we asked participants to explain, in their own words, how they made their decisions during the experiment (**Supplementary Table 9**). No participant mentioned concerns about their reputation or reciprocity, while 86% of participants used language indicative of value computation (for example, "worth", "value", "calculate"). Only 7% of participants mentioned concerns about the pain tolerance of the receiver.

**Moral decision task.** On each trial, deciders had to choose between two options involving pairs of numbers of shocks and amounts of money: a harmful option containing more shocks and money, and a helpful option containing fewer shocks and less money. The decider always received the money, but the shocks were allocated to the decider in half of the trials (Self condition) and to the receiver in the other half (Other condition). Deciders had a maximum of 6 s to select either the left or right side option by pressing a button box with their left or right index finger. Button presses resulted in the selected option being highlighted for the remainder of the 6-s decision period. If a response was not made within 6 s, the missed trial was repeated at the end of the session. Transitions between conditions were cued with an instruction screen lasting 2 s. Each trial culminated in an intertrial interval jittered between 1 and 6 s. Participants completed a total of 216 trials, delivered across two scanning runs lasting approximately 20 min each. To avoid habituation and preserve choice independence, no money or shocks were delivered during the task. Instead, one trial was randomly selected and implemented at the end of the experiment. All procedures were fully transparent to participants, and no deception was used in the paradigm.

Our trial set was optimized to jointly satisfy two constraints. First, we aimed to optimize the trials to give the most efficient estimates of potential participants' harm aversion parameters  $\kappa_{\text{self}}$  and  $\kappa_{\text{other}}$ . Second, we aimed to decorrelate, across trials, the relative amounts of profit and pain that would result from participants' choices. We satisfied the first constraint using a procedure described in detail elsewhere<sup>15</sup> to create a set of 54 trials that efficiently estimated participants' harm-aversion parameters. We then repeated this procedure 10,000 times. For each iteration, we simulated choices on the trial set across a range of values of  $\kappa_{\text{self}}$  and  $\kappa_{\text{other}}$ , computed the correlations between the amounts of profit and pain resulting from simulated choices and selected the trial set that resulted in the lowest correlation between parameters. After creating this optimized trial set, we duplicated it and reversed the left and right options, producing a full set of 108 trials. Participants completed each of these 108 trials in both the Self condition and the Other condition, for a total of 216 trials. Thus, each money/shock pair appeared four times: twice in each condition (Self/Other) and twice on each side (left/right). We created four different trial sequences that each contained an equal number of Self- and Other-trials in the first and second blocks of 108 trials, and participants were randomly assigned to receive one of the four trial sequences.

The trial optimization procedure successfully satisfied our constraints: across trials, the amounts of profit and pain that would result from choosing the more harmful option were uncorrelated ( $r = 0.009$ ,  $P = 0.926$ ; **Fig. 1b**). In addition, there were no significant correlations between the relative and total number of shocks across the two options ( $r = -0.02$ ,  $P = 0.84$ ) nor between the relative and total amounts of money across the two options ( $r = -0.13$ ,  $P = 0.18$ ). Across participants, relative and total subjective values were also not significantly correlated ( $r = -0.14$ ,  $P = 0.15$ ). This suggests our findings related to relative values are unlikely to be explained by total value.

**Moral blame task.** Participants evaluated sequences of 30 moral decisions made by two fictional agents, presented in random order, for a total of 60 trials. Trials were self-paced. On each trial, agents faced a choice similar to that faced by deciders in the fMRI study, i.e., they had to choose between delivering more painful electric shocks to another person for a larger profit or delivering fewer shocks but for a smaller profit. We used our model of moral decision-making<sup>15</sup> to simulate the choices of a bad agent with  $\kappa_{\text{other}} = 0.3$ , who mostly chose the harmful option, and a good agent with  $\kappa_{\text{other}} = 0.7$ , who mostly chose the helpful option. After observing each choice, participants provided a moral judgment of the choice on a continuous visual analog scale ranging from 0 (blameworthy) to 1 (praiseworthy; **Supplementary Fig. 1**). Across trials, we independently manipulated the amounts of profit and pain resulting from the agent's choices, which enabled us to examine how profit and pain resulting from harmful choices load onto blame judgments.

**fMRI acquisition and preprocessing.** fMRI scanning was performed on a 3-Tesla Siemens Allegra scanner with a Siemens head coil, at the Wellcome Trust Centre for Neuroimaging at University College London. Functional images were taken with a gradient echo T2\*-weighted echo-planar sequence (repetition time = 3.36 s, echo time = 30 ms, flip angle = 90°, 64 × 64 matrix, field of view = 192 mm, slice thickness = 2 mm with 1-mm gap). A total of 40 axial slices were acquired in ascending order (in-plane resolution 3 × 3 mm). We acquired 428 volumes in



each of two sessions, and the initial five volumes of each session were discarded to allow for steady-state magnetization. Slices were tilted at an orientation of  $-30^\circ$  to minimize signal dropout in ventral frontal cortex. Anatomical images were T1-weighted (MDEFT,  $1 \times 1 \times 1$  mm resolution). We also acquired a field map (double-echo FLASH, short TE = 10 ms, long TE = 12.46 ms,  $3 \times 3 \times 3$  mm resolution with 1-mm gap) to correct distortions in the functional images. We used a breathing belt and pulse oximeter to collect physiological data during the imaging sessions.

All image preprocessing and analysis was carried out in SPM8 (Wellcome Department of Imaging Neuroscience). Images were realigned to the first scan of the first session and unwarped using field maps, spatially normalized via segmentation of the T1 structural image into gray matter, white matter and CSF using ICBM tissue probability maps, and spatially smoothed with a Gaussian kernel (8-mm full-width at half-maximum).

**GLM1: model of relative chosen value.** We constructed a GLM to identify regions responding parametrically at decision onset to the subjective value of the chosen and unchosen options, as determined by our computational model of choice. We regressed fMRI time-series onto a GLM containing four main event regressors describing the onsets of (i) Self trials in which the left option was selected; (ii) Self trials in which the right option was selected; (iii) Other trials in which the left option was selected; and (iv) Other trials in which the right option was selected. All four events were modeled with a duration corresponding to the participant's RT on that trial and were each associated with two parametric modulators: the subjective value of the chosen and unchosen options, derived from each participant's choice model. Critically, custom scripts ensured that these two parametric modulators competed for variance during the estimation, rather than being serially orthogonalized as is standard in SPM. The GLM contained four additional event regressors of no interest, describing the onsets of: (i) left button presses; (ii) right button presses; (iii) screen signaling transition to the Self condition; and (iv) screen signaling transition to the Other condition. These events were modeled as stick functions with duration zero. Finally, a total of 23 nuisance regressors were included to control for motion and physiological effects of no interest. These included the six motion regressors obtained during realignment, as well as 17 physiological regressors derived from a physiological noise model, constructed using an in-house Matlab toolbox<sup>48</sup>: ten for cardiac phase, six for respiratory phase and one for respiratory volume.

**GLM2: model of decision parameters.** We built a GLM to identify regions responding parametrically at decision onset, irrespective of participants' choices, to the objective amounts of profit and pain that would result from choosing the harmful option relative to the helpful option in the Self and Other conditions. We regressed fMRI time-series onto a GLM containing four main event regressors describing the onsets of (i) Self trials in which the left option was selected; (ii) Self trials in which the right option was selected; (iii) Other trials in which the left option was selected; and (iv) Other trials in which the right option was selected. All four events were modeled with a duration corresponding to the participant's RT on that trial and were each associated with four parametric modulators: the amount of profit and pain for the harmful and the helpful option, irrespective of what the participant chose. Again we ensured that these four parametric modulators competed for variance during the estimation. There were four additional event regressors of no interest, indicating the onsets of button presses and transitions between task conditions, as well as 23 nuisance regressors controlling for motion and physiological effects of no interest.

**GLM3–GLM6: ROI analysis in LPFC.** To test different accounts of the role of LPFC in moral decision-making, we extracted time-course data from a 4-mm sphere surrounding independently defined ROI coordinates in LPFC. Because we were interested in moral decisions we restricted these analyses to trials in the Other condition. Custom Matlab scripts were used to orthogonalize each participant's time-series with respect to motion and physiological regressors and to apply a high-pass filter. The time-series were then normalized, up-sampled at 100 ms and time-locked to decision onsets, creating a data matrix with dimensions  $n_{\text{trials}} \times n_{\text{timepoints}}$ . Next, we fit a GLM across trials separately for each participant, resulting in parameter estimates at each time point for each GLM regressor. To test the significance of each regressor in LPFC, we convolved the regressor time series with a canonical hemodynamic response function aligned to decision

onset and calculated the resulting  $t$  statistics and  $P$  values. The latency for the canonical hemodynamic response function was estimated using the CANlab Core Tools package<sup>49</sup>.

We tested four GLMs in LPFC using the above procedure.

$$\text{GLM3: } y = B_1 \times v_{\text{diff}} + B_2 \times v_{\text{tot}} + B_3 \times \text{blame} + e;$$

$$\text{GLM4: } y = B_1 \times v_{\text{diff}} + B_2 \times m_{\text{tot}} + B_3 \times s_{\text{tot}} + B_4 \times \text{blame} + e;$$

$$\text{GLM5: } y = B_1 \times \text{help} + B_2 \times v_{\text{diff}} + B_3 \times v_{\text{tot}} + B_4 \times \text{blame} + e; \text{ and}$$

$$\text{GLM6: } y = B_1 \times v_{\text{help}} + B_2 \times v_{\text{harm}} + B_3 \times v_{\text{help}} \times \text{help} + B_4 \times v_{\text{harm}} \times \text{help} + B_5 \times v_{\text{diff}} + e;$$

where  $v_{\text{diff}}$  refers to relative chosen value (i.e., the value of the chosen option relative to the unchosen option),  $v_{\text{tot}}$  refers to sum of the values of the chosen and unchosen options,  $m_{\text{tot}}$  refers to the total amount of money available on a trial,  $s_{\text{tot}}$  refers to the total number of shocks available on a trial,  $v_{\text{harm}}$  refers to the value of the harmful option,  $v_{\text{help}}$  refers to the value of the helpful option and  $e$  denotes an error term. Value and blame regressors were computed individually for each participant based on their individual preference parameters as estimated from the moral decision model.

**PPI model: functional connectivity with LPFC.** We created LPFC seed regressors by computing individual average time series within 4-mm spheres surrounding individual subject peaks within the functional masks of left LPFC as shown in **Figure 2a**. The locations of the peak voxels were based on the GLM2 contrast, showing parametric effects of profit resulting from choosing the more harmful option in the Other condition relative to choosing it in the Self condition. Variance associated with the six motion regressors was removed from the extracted time-series. To construct a time-series of neural activity in the left LPFC, the seed time-courses were deconvolved with the canonical hemodynamic response function. We then estimated the first PPI model (PPI1) with the following regressors: (i) an interaction between the neural activity in LPFC and a vector coding for the main effect of decision type (1 for help-other,  $-1$  for harm-other); (ii) the main effect of decision type; and (iii) the original BOLD eigenvariate (i.e., the average time-series from the LPFC seed), as well as the six motion parameters as regressors of no interest. We also estimated a second, complementary PPI model (PPI2) that was identical to the first model except that the first regressor contrasted decisions to help other with decisions to help self (1 for help-other,  $-1$  for help-self).

**Statistical analyses.** We used a within-subjects design, so experimental group randomization and blinding were not applicable. Data analysis was not performed blind to the conditions of the experiments. We analyzed behavioral data using  $t$  tests and multiple linear regressions. We analyzed fMRI data using mass univariate methods implemented in SPM8. At the first level, we implemented linear regression at each voxel, using generalized least-squares with a global approximate AR(1) autocorrelation model, drift-fit with a discrete cosine transform basis (128-s cutoff). At the second level, we implemented linear regression at each voxel, using ordinary least-squares. All Student's  $t$  tests were two-tailed. For correlations between brain responses and moral preferences, we report the percentage bend correlation, which is robust to outliers, using the Matlab robust correlation toolbox<sup>50</sup>. The toolbox uses the 95% bootstrap confidence interval rather than  $P$  values to make statistical inferences, because the 95% confidence interval is less affected by heteroscedasticity than the traditional  $t$  test.

**Moral decision task: choices.** We analyzed the moral decision data with a model based on previous studies using the moral decision task<sup>15,16</sup> that explained choices in terms of the value difference ( $\Delta V$ ) between the harmful and helpful options. As the fMRI task required participants to select between two alternatives on each trial, rather than switch from a default to an alternative option as in previous studies, we omitted the loss-aversion parameter from the model here. Trial-by-trial value differences were transformed into choice probabilities using a softmax function<sup>35</sup>:

$$P(\text{choose alternative}) = \left( \frac{1}{1 + e^{-\gamma \Delta V}} \right)$$

where  $\gamma$  is a subject-specific inverse-temperature parameter that characterizes the sensitivity of choices to  $\Delta V$ . We optimized participant-specific parameters across trials using nonlinear optimization implemented in Matlab (MathWorks) for maximum likelihood estimation. Parameters were estimated individually for

each participant, and summary statistics were calculated from these parameter estimates at the group level, treating each parameter estimate as a random effect<sup>51</sup>. Parametric statistics were used to compare harm aversion for self and others as these parameters were normally distributed (Kolmogorov-Smirnov test for  $\kappa_{\text{other}} = 0.097$ ,  $P = 0.2$ ; for  $\kappa_{\text{self}} = 0.107$ ,  $P = 0.2$ ). See **Supplementary Modeling Note** and **Supplementary Software** for details.

**Moral decision task: RTs.** We analyzed RT data using a GLM (RT-GLM1) that regressed RTs during the Other condition against the following regressors: (i) dummy indicating helpful versus harmful choices; (ii) unsigned value difference; (iii) total value; and (iv) maximum number of shocks. In a second GLM (RT-GLM2) we regressed RTs during all conditions against the following regressors: (i) dummy indicating Self versus Other condition; (ii) unsigned value difference; (iii) total value; and (iv) maximum number of shocks. We optimized participant-specific parameters across trials using the 'glmfit' procedure in Matlab. Parameters were estimated individually for each participant, and summary statistics were calculated from these parameter estimates at the group level, treating each parameter estimate as a random effect<sup>51</sup>. See **Supplementary Table 7** and **Supplementary Software** for details.

**Moral blame task.** We analyzed the moral blame data using a GLM that regressed participants' z-scored blame judgments onto the amounts of profit and pain resulting from harmful decisions (relative to helpful decisions) as well as individual preference parameters ( $\kappa_{\text{self}}$ ,  $\kappa_{\text{other}}$ ) estimated from the moral decision model. We also estimated a second, reduced model that included terms for profit and pain only. Because we were primarily interested in blame judgments for harmful choices, we restricted this analysis to trials on which the bad agent chose the harmful option. Group-level parameters were estimated using the regress function in Matlab. We report *F* statistics and *P* values from the full models as well as parameter estimates and 95% confidence intervals for each model in the **Supplementary Modeling Note**. We used the blame model, estimated on data from the behavioral study, to create a unique blame regressor for each participant in the fMRI study (Fig. 3a). These were computed by applying the parameters from the blame model to the amounts of profit and pain in the fMRI trials and to the fMRI participants' preference parameters  $\kappa_{\text{self}}$  and  $\kappa_{\text{other}}$ . The blame regressors were used in GLM3–GLM5. See **Supplementary Modeling Note** and **Supplementary Software** for details.

**fMRI: correction for multiple comparisons.** For whole-brain analyses, we tested for statistical significance using whole-brain correction ( $P < 0.05$ , FWE-corrected at the cluster level after voxel-wise thresholding at  $P < 0.001$ ). This threshold provides an acceptable FWE control<sup>52</sup>. *Post hoc* analyses of regions identified in the whole-brain analyses were carried out using one-sample *t* tests on mean signal extracted from 4-mm spheres surrounding independently defined ROIs (**Supplementary Table 2**). For ROI analyses, mean signal was extracted from 4-mm spheres surrounding coordinates defined from previous studies. For analyses in TPJ, ACC and insula, we took coordinates from previous meta-analyses of empathy for pain and moral judgment<sup>19,53</sup>. For analyses in LPFC, we took the mean of peak coordinates from previous studies investigating LPFC modulation of subjective value signals<sup>54–58</sup>. For analyses in DS, we took coordinates from an anatomical study of corticostriatal connectivity<sup>33</sup>. Images are displayed at a threshold of  $P < 0.005$ ,  $k > 10$  to show the extent of activation in significant clusters. Results are reported using the MNI coordinate system.

**fMRI: PPI analysis.** For the LPFC connectivity analysis we tested for statistical significance by conducting a conjunction analysis of the PPI contrasts from PPI1 and PPI2. To compute an appropriate threshold for the two-way conjunction of contrasts, we employed Fisher's method<sup>59</sup>, a procedure that combines probabilities of multiple hypothesis tests using the following formula:

$$\chi^2 = -2 \sum_{i=1}^k \log_e(p_i)$$

where  $p_i$  is the *P*-value for the *i*th test being combined,  $k$  is the number of tests to be combined and the resulting statistic has a  $\chi^2$  distribution with  $2k$  degrees of freedom. Using this method, thresholding each contrast at  $P = 0.01$  resulted in a combined threshold of  $P < 0.001$ , uncorrected. We report as significant all those results surviving whole-brain correction for multiple comparisons (cluster-level corrected after voxel-wise thresholding at  $P < 0.001$ ).

A **Supplementary Methods Checklist** is available.

**Data availability.** The data that support the findings of this study are available from the corresponding author upon reasonable request.

**Code availability.** Analysis code for fitting models to moral decision task choice data, moral decision task RT data and blame judgment data are provided as **Supplementary Software**. All other analysis code is available from the corresponding author upon reasonable request.

48. Hutton, C. *et al.* The impact of physiological noise correction on fMRI at 7 T. *Neuroimage* **57**, 101–112 (2011).
49. Lindquist, M.A., Meng Loh, J., Atlas, L.Y. & Wager, T.D. Modeling the hemodynamic response function in fMRI: efficiency, bias and mis-modeling. *Neuroimage* **45** (Suppl. 1), S187–S198 (2009).
50. Pernet, C.R., Wilcox, R. & Rousselet, G.A. Robust correlation analyses: false positive and power validation using a new open source matlab toolbox. *Front. Psychol.* **3**, 606 (2013).
51. Holmes, A. & Friston, K. Generalisability, random effects & population inference. *Neuroimage* **7**, S754 (1998).
52. Flandin, G. & Friston, K.J. Analysis of family-wise error rates in statistical parametric mapping using random field theory. Preprint at <https://arxiv.org/abs/1606.08199> (2016).
53. Bzdok, D. *et al.* Parsing the neural correlates of moral cognition: ALE meta-analysis on morality, theory of mind, and empathy. *Brain Struct. Funct.* **217**, 783–796 (2012).
54. Hare, T.A., Camerer, C.F. & Rangel, A. Self-control in decision-making involves modulation of the vmPFC valuation system. *Science* **324**, 646–648 (2009).
55. Rudolf, S. & Hare, T.A. Interactions between dorsolateral and ventromedial prefrontal cortex underlie context-dependent stimulus valuation in goal-directed choice. *J. Neurosci.* **34**, 15988–15996 (2014).
56. Hare, T.A., Malmaud, J. & Rangel, A. Focusing attention on the health aspects of foods changes value signals in vmPFC and improves dietary choice. *J. Neurosci.* **31**, 11077–11087 (2011).
57. Hare, T.A., Hakimi, S. & Rangel, A. Activity in dlPFC and its effective connectivity to vmPFC are associated with temporal discounting. *Front. Neurosci.* **8**, 50 (2014).
58. Maier, S.U., Makwana, A.B. & Hare, T.A. Acute stress impairs self-control in goal-directed choice by altering multiple functional connections within the brain's decision circuits. *Neuron* **87**, 621–631 (2015).
59. Fisher, R.A. *Statistical Methods for Research Workers* (Genesis Publishing, 1925).